

## “Amorphous Nickel Sulfide” Is Hydrated Nanocrystalline NiS with a Core–Shell Structure

Shanshan Huang,<sup>†,‡</sup> Kenneth D. M. Harris,<sup>\*,§</sup> Elisa Lopez-Capel,<sup>⊥</sup> David A. C. Manning,<sup>⊥</sup> and David Rickard<sup>\*,†</sup>

<sup>†</sup>*School of Earth and Ocean Sciences, Cardiff University, Cardiff CF10 3YE, Wales,* <sup>§</sup>*School of Chemistry, Cardiff University, Cardiff CF10 3AT, Wales,* and <sup>⊥</sup>*School of Civil Engineering and Geosciences, University of Newcastle upon Tyne, Newcastle upon Tyne NE1 7RU, England.* <sup>\*</sup>*Present address: Centre for Geobiology and Department of Earth Sciences, University of Bergen, Allégaten 41, Bergen 5007, Norway.*

Received July 29, 2009

The application of a range of experimental techniques shows that “amorphous nickel sulfide” (the material precipitated from aqueous solutions of Ni<sup>II</sup> salts and S<sup>II-</sup> under ambient conditions) is actually a hydrated nanoparticulate material with an approximate formula NiS · 1.5H<sub>2</sub>O. The particles comprise a crystalline, anhydrous core (diameter ca. 1–3 nm) with the millerite (NiS) structure, surrounded by a hydrated shell phase. The materials prepared under acidic conditions (pH = 3 and 5) transform with age to form polydymite (Ni<sub>3</sub>S<sub>4</sub>) and heazlewoodite (Ni<sub>3</sub>S<sub>2</sub>), while materials prepared at pH = 7 and 9 do not undergo this transformation. At pH = 12, the preparation procedure yields NiAs-type NiS as a metastable phase.

Thiel and Gessner<sup>1</sup> pioneered the study of “amorphous nickel sulfide”, and this material was also reported recently<sup>2</sup> in the synthesis of nickel sulfides from aqueous solution. However, no detailed structural analysis of “amorphous nickel sulfide” has been reported. In the present work, we have carried out a comprehensive investigation of the structural and compositional properties of this material by employing a range of experimental techniques. Our nickel sulfide materials were prepared<sup>3,4</sup> (see the Supporting Information) under ambient conditions (ca. 20 °C, 0.1 MPa) by reaction between aqueous NiSO<sub>4</sub> and Na<sub>2</sub>S at different values of pH in the range 3–12. As shown in Figure 1a for the material prepared at pH = 7, the powder X-ray diffraction (XRD) patterns of these materials typically exhibit only broad scattering features, with no discrete Bragg peaks

observed. Analysis of the X-ray scattering data is discussed below.

Fringes observed in high-resolution transmission electron microscopy (HRTEM) data (Figure 2) confirm that the nickel sulfide materials are nanocrystalline and indicate that the particles are anhedral with sizes of ca. 2–9 nm. The intrafringe spacings are dominated by distances of 1.9 and 2.2 Å, representing 54% and 32%, respectively, of the 72 fringes measured for materials prepared for pH in the range 3–9. Among the possible nickel sulfide phases, only millerite has *d* spacings close to 1.9 and 2.2 Å [(131) and (211) planes, respectively]. The dominant intrafringe distances observed in the HRTEM images are attributed to a preferred particle shape and orientation. Selected area electron diffraction (SAED) patterns typically comprise spotty rings (Figure 2), suggesting that the materials are polycrystalline on the length scale probed by the electron beam, representing small domain sizes consistent with the nanocrystalline assignment of the particle size discussed above. Most of the 21 SAED patterns studied for materials prepared for pH = 3–9 match the positions of the reflections for millerite.

To establish structural information from the X-ray scattering data, pair distribution function (PDF) analysis<sup>5,6</sup> was performed on data recorded (for the materials prepared at pH = 3–9 and aged for 16 days) at the SPring-8 synchrotron radiation facility (Figure 1). The results show a well-defined nearest-neighbor distance of ca. 2.3 Å, with the PDF peaks diminishing by ca. 10 Å, consistent with the structural coherence of the materials being on the nanoscale. Refinement of the PDF data was attempted for 10 different structural models based on the seven known nickel sulfide phases and other plausible structures. From the quality of the fits obtained for all structural models (see the Supporting Information), the polydymite, millerite, and nickel pentlandite structures give significantly superior fits to the PDF data and are essentially indistinguishable from each other.

\*To whom correspondence should be addressed. E-mail: rickard@cardiff.ac.uk (D.R.), harriskdm@cardiff.ac.uk (K.D.M.H.).

(1) Thiel, A.; Gessner, H. *Z. Anorg. Chem.* **1914**, *86*, 1–57.

(2) Jeong, Y. U.; Manthiram, A. *Inorg. Chem.* **2001**, *40*, 73–77.

(3) While we use pH as a convenient means of labeling the samples prepared under different conditions, we emphasize that we are not implying that materials prepared at the same pH by other preparation procedures (e.g., in the presence of other foreign ions in solution) must necessarily have the same properties as those reported here.

(4) We note that, in repeated preparations under the same conditions, the properties of the materials obtained are found to be reproducible.

(5) (a) Egami, T.; Billinge, S. J. L. *Underneath the Bragg Peaks: Structural Analysis of Complex Materials*; Pergamon, Cambridge, U.K., 2003. (b) Billinge, S. J. L.; Kanatzidis, M. G. *Chem. Commun.* **2004**, 749–760.

(6) Billinge, S. J. L.; Levin, I. *Science* **2007**, *316*, 561–565.

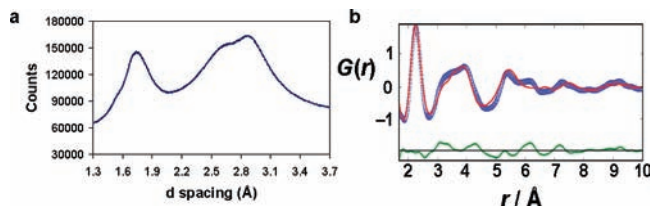


**Figure 1.** (a) Synchrotron powder XRD pattern for the material prepared at pH = 7 (aged for 16 days). (b) Best fit ( $R_w = 0.24$ ) obtained in the PDF analysis for the millerite model from the same experimental data (blue, experimental data; red, calculated data; green, difference plot). The pair distribution function  $G(r)$  (where  $r$  represents distance) is defined in ref 5.

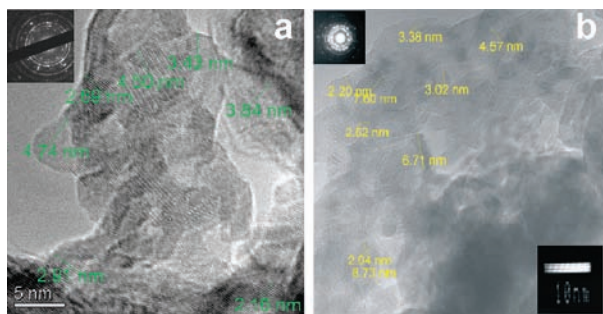


**Figure 2.** HRTEM images for materials prepared at (a) pH = 3, and (b) pH = 9 (aged for 23 days in each case), showing anhedral crystals with dimensions of ca. 2–9 nm.

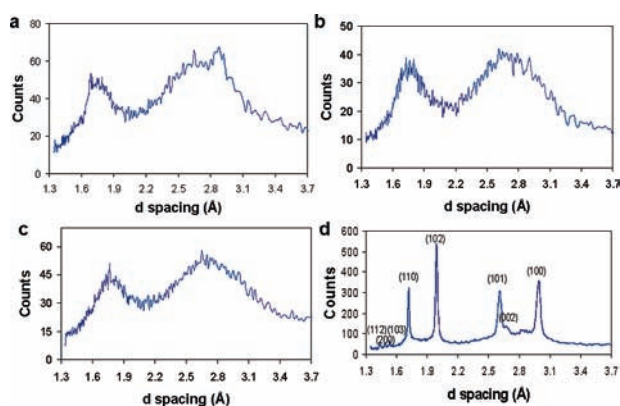


**Figure 3.** Powder XRD patterns for the materials prepared at (a) pH = 3, (b) pH = 5, (c) pH = 9, and (d) pH = 12 and aged for 4 days in each case.

Thus, the structure is not assigned uniquely on the basis of the PDF analysis alone. However, as discussed above, analysis of SAED and HRTEM data supports the assignment of the millerite structure, consistent with one of the models that gives a good quality of the fit to the PDF data.

The effect of the preparation pH on the structural properties is assessed from Figure 3, which shows that the powder XRD patterns of materials prepared for pH = 3–9 (aged for 4 days) are essentially identical. Thus, structural analysis from these data would lead to the same conclusions discussed above for pH = 7. The material prepared at pH = 12 is substantially more crystalline than those prepared at lower pH and has the NiAs structure type. We note that NiAs-type NiS is a high-temperature form of nickel sulfide.<sup>7</sup>

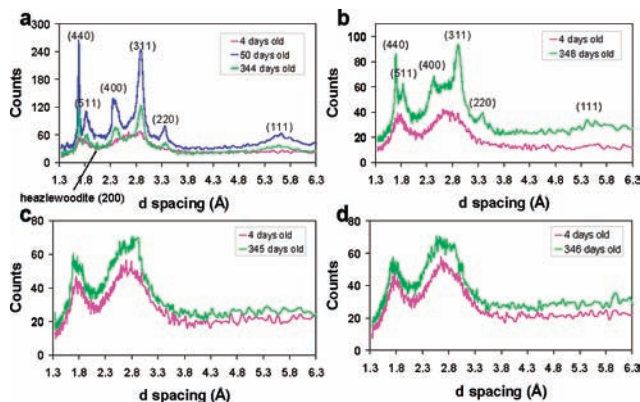


**Figure 4.** Powder XRD patterns of materials prepared at (a) pH = 3, (b) pH = 5, (c) pH = 7, and (d) pH = 9 as a function of age. In parts a and b, reflections due to polydymite develop with age. In part a, a low-intensity peak assigned as heazlewoodite (200) is also clearly identified. In parts c and d, no significant changes in the pattern are observed with age.

Powder XRD patterns of the materials prepared for pH = 3–9 are shown in Figure 4 as a function of age after preparation. The materials are initially nanocrystalline and show X-ray scattering patterns similar to that discussed above (Figure 1a) for pH = 7. However, the materials prepared under acidic conditions (pH = 3 and 5) transform as a function of age, leading to powder XRD patterns that have sharper Bragg maxima in positions characteristic of polydymite ( $\text{Ni}_3\text{S}_4$ ). For the material prepared at pH = 3, polydymite with high crystallinity is observed within 50 days, whereas for the materials prepared at pH = 7 and 9, the original powder XRD pattern remains for at least 1 year. SAED experiments on a sample prepared at pH = 3 and aged for 241 days reveal that heazlewoodite ( $\text{Ni}_3\text{S}_2$ ) is also produced in this transformation [the  $(1\bar{1}0)$ ,  $(1\bar{1}1)$ ,  $(200)$ , and  $(0\bar{1}2)$  reflections of heazlewoodite are clearly observed]. The powder XRD pattern of the material prepared at pH = 3 and aged for 344 days has a low-intensity peak at 2.0 Å, which can only be assigned as heazlewoodite (200). These observations suggest that the overall transformation is



Chemical analyses of the nanoparticulate materials were carried out following dissolution in acid. Sulfur was analyzed using the method of Rickard et al.,<sup>8</sup> and nickel was analyzed by inductively coupled plasma optical emission spectroscopy. After freeze-drying for 48 h, the materials appeared dry. However, the analytical totals of Ni and S average only  $78.6 \pm 2.2$  wt %, suggesting that ca. 21 wt % water may be present. From independent analyses using ion chromatography and energy-dispersive X-ray analysis (on an electron microscope), no significant amounts of any other cations or anions were found. The analytical totals show no systematic trends and are not related to the age or the total amount of the sample. The addition of  $\text{CrCl}_2$  (as a reducing agent) in the dissolution process did not change the measured composition, and the samples dissolved readily with or without  $\text{CrCl}_2$ . The Ni:S ratio corresponds to an excess of Ni over S in the bulk material (by an amount greater than the analytical uncertainty), varying from 1.03 to 1.11 (average, 1.07).

(7) Kullerud, G.; Yund, R. A. *J. Petrol.* **1962**, *3*, 126–175.

(8) Rickard, D.; Griffith, A.; Oldroyd, A.; Butler, I. B.; Lopez-Capel, E.; Manning, D. A. C.; Apperley, D. C. *Chem. Geol.* **2006**, *235*, 286–298.

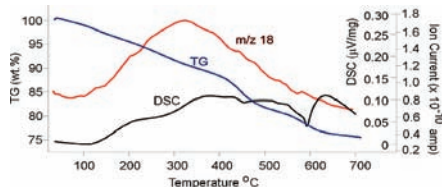


**Figure 5.** TGA–MS data for heating the material prepared at pH = 9 from 30 to 700 °C. The mass loss is attributed to water (see the evolution of  $m/z = 18$  in the MS analysis). DSC shows a weak exothermic process. The endothermic peak at ca. 600 °C is ascribed to a phase change.

Combined thermogravimetric and mass spectral analysis (TGA–MS) on heating the nanoparticulate materials (prepared at pH = 9) shows a mass loss of ca. 22.5 wt % in the temperature range up to ca. 600 °C, assigned (from the MS analysis) as loss of water (Figure 5). The differential scanning calorimetry (DSC) trace shows two endotherms corresponding to inflections in the mass loss curve at ca. 450 and 600 °C.

The mass percentage of water determined by TGA–MS is consistent with the amount of water deduced from the wet chemical analyses. A millerite standard (99.9% NiS) of high crystallinity showed a mass loss of less than 1% in TGA–MS experiments between 30 and 500 °C. Isothermal TGA–MS studies of the nanoparticulate materials at 200 °C as a function of the time showed a total mass loss of only ca. 4%, with the mass loss leveling off at the end of the 2 h experiment, suggesting that the majority of the water is not surface-adsorbed water but is instead integral to the structure of the material. The broad peak for water evolution suggests that the water molecules have a distribution of environments. There is no significant change in the water content upon storage of the materials in an anoxic environmental chamber for 60 days. From these results, the stoichiometry of the nanoparticulate nickel sulfides is represented approximately as NiS · 1.5H<sub>2</sub>O. We note that similar preparation procedures for iron sulfide (FeS) yield nanoparticulate materials in which no water is present.<sup>8</sup>

Our combined evidence suggests that the structure of the hydrated nickel sulfide nanoparticles is described by the type of model proposed for hydrated ZnS nanoparticles by Zhang et al.<sup>9</sup> From our HRTEM data, the average particle size is ca. 4 nm and ranges from ca. 2 to 9 nm. Particle size refinement in the PDF analysis gives values in the range ca. 1–3 nm for samples prepared in the pH range 3–9 (typically with lower particle size for materials prepared at higher pH). These observations suggest a model of nanoparticles comprising an anhydrous crystalline NiS core (diameter ca. 1–3 nm) with the millerite structure, surrounded by a fairly robust shell phase with a thickness on the order of a few nanometers (corresponding to total particle diameters typically in the region of ca. 4 nm and up to a maximum of ca. 9 nm, as observed from the HRTEM data). The shell phase contains

water and is assumed to be the origin of the variable nickel content, but the structural coherence of the shell region is considerably lower than that of the core region. Clearly, further research is required to establish structural details of the shell region and of the interface between the core and shell regions. In particular, computer simulation studies may be a particularly powerful approach for establishing more detailed insights on these issues. It is also relevant to consider whether the water component of the shell region may be replaced by other molecules via alternative preparation conditions.

The transformation from millerite to polydymite upon aging of the nanoparticulate materials is deduced to be a solid-state process because freeze-dried materials kept under standard conditions in an anoxic chamber are observed to transform to polydymite. The higher rate of this transformation for materials prepared at lower pH suggests that the water in the nanoparticles retains part of the proton balance of the original solution. The transformation from millerite (NiS) to polydymite (Ni<sub>3</sub>S<sub>4</sub>) is analogous to the reported solid-state transformation of FeS (mackinawite) to Fe<sub>3</sub>S<sub>4</sub> (greigite).<sup>10</sup> Our finding that heazlewoodite (Ni<sub>3</sub>S<sub>2</sub>) is also formed in the transformation from millerite to polydymite suggests a possible explanation for the problem of the electron balance in the transformation from FeS to Fe<sub>3</sub>S<sub>4</sub>.<sup>10</sup>

The formation of NiAs-type NiS (a high-temperature form of NiS) at pH = 12 under ambient conditions is analogous to the formation of hexagonal ZnS (wurtzite) in aqueous solution.<sup>11</sup> The stable form of ZnS under ambient conditions is sphalerite (wurtzite is stable only above 1100 °C). Luther et al. have shown<sup>11</sup> that wurtzite forms as a metastable phase at low temperature when the aqueous ZnS clusters that immediately precede its precipitation have a hexagonal structure. The formation of NiS with the metastable NiAs structure in the experiments reported here at pH = 12 is likely to result from an analogous process.

**Acknowledgment.** S.H. was funded by a Dorothy Hodgkin Postgraduate Fellowship supervised by D.R. We thank Z. Yao and H. Ohfuji (for help with TEM), M. Takata (for providing the opportunity to record X-ray scattering data at SPring-8), K. Kato (for measuring data at SPring-8), S. Kohara (for the initial processing of the data for PDF analysis), A. Oldroyd (for advice on preparative aspects), and T. Proffen (for advice on PDF analysis).

**Supporting Information Available:** Experimental details for sample preparation, elemental analyses, thermal analysis, X-ray scattering data collection, HRTEM experiments, PDF analysis, and information about the 10 structural models used in the analysis of the XRD, HRTEM, and SAED data. This material is available free of charge via the Internet at <http://pubs.acs.org>.

(10) Rickard, D.; Luther, G. W. *Chem. Rev.* **2007**, *107*, 514–562.

(11) Luther, G.; Theberge, S.; Rickard, D. *Geochim. Cosmochim. Acta* **1999**, *63*, 3159–3169.

(9) Zhang, H.; Gilbert, B.; Huang, F.; Banfield, J. F. *Nature* **2003**, *424*, 1025–1029.